DOI: 10.1021/ic900899j

Inorganic Chemistry
Article

Photosensitization of Ruthenium Nitrosyls to Red Light with an Isoelectronic Series of Heavy-Atom Chromophores: Experimental and Density Functional Theory Studies on the Effects of O-, S- and Se-Substituted Coordinated Dyes

Michael J. Rose and Pradip K. Mascharak*

Department of Chemistry and Biochemistry, University of California Santa Cruz, Santa Cruz, California 95064

Received May 8, 2009

Three ruthenium nitrosyl-dye conjugates, namely, [((OMe)$_2$bQb)Ru(NO)(Resf)] (**RuNO-Resf**), [((OMe)$_2$bQb)Ru(NO)(Thnl)] (**RuNO-Thnl**), and [((OMe)$_2$bQb)Ru(NO)(Seln)] (**RuNO-Seln**) have been synthesized using the tetradentate N4 dicarboxamido ligand H$_2$(OMe)$_2$bQb. Each nitrosyl of this series is conjugated to a phenoxazine-type heterotricyclic chromophore which has been systematically varied in a central position to test the effects of "heavy-atom" substitution (O = Resorufin; S = Thionol; Se = Selenophore) in photosensitization. The structure of the chloride-bound precursor {Ru-NO}^{6} nitrosyl [((OMe)$_2$bQb)Ru(NO)(Cl)] (**RuNO-Cl**) and three nitrosyl-dye conjugates, namely, **RuNO-Resf**, **RuNO-Thnl** and **RuNO-Seln**, have been determined by X-ray crystallography. All three nitrosyl-dye conjugates exhibit sharp ^{1}H NMR spectra ($S = 0$ ground state) and ν_{NO} stretches in the IR spectrum in the region 1825−1855 cm^{-1}, typical of {Ru-NO}^{6} nitrosyls. The presence of a heavy atom in the bound dye gives rise to a systematic red-shift in the electronic absorption spectrum, shifting from **RuNO-Resf** (λ_{max} = 500 nm) to **RuNO-Thnl** (λ_{max} = 530 nm) to **RuNO-Seln** (λ_{max} = 535 nm). Results of careful measurements with monochromatic light sources indicate that heavy-atom substitution in the coordinated dye makes the resulting nitrosyl-dye conjugates more susceptible to light of longer wavelength (lower energy). Density functional theory (DFT) calculations on **RuNO-Cl**, **RuNO-Resf**, **RuNO-Thnl**, and **RuNO-Seln** have been performed to gain insight into the electronic structure of the {dye-Ru-NO} frame and the nature of transition(s) that sensitizes these conjugates to lights of longer wavelengths and promote NO photolability. Results of this study provide an explanation for the sensitization observed in our strategy of direct attachment of dye molecules to {Ru-NO}^{6} nitrosyls. This strategy could lead to eventual isolation of designed metal nitrosyls that are sensitive to red- or near-infrared light and hence potential photodynamic therapy (PDT) agents for treatment of malignancies with high doses of NO.

Introduction

Nitric oxide (NO) has been shown to play key roles in a number of biological processes including blood pressure regulation, neurotransmission and inflammatory host response.[1,2] More recently, NO has drawn attention for its ability to elicit apoptosis in cells via biological activation of the caspase death-signaling pathway[3] and chemical inhibition of enzymes involved in mitrochondrial respiration.[4] Since elevated concentrations (μM or higher) of NO induce apoptosis,[5] many researchers have sought to deliver NO selectively to malignant sites as a potential means of killing cancer cells.[6,7] A number of exogenous organic

*To whom correspondence should be addressed. E-mail: pradip@chemistry.ucsc.edu. Phone: (831) 459-5251. Fax: (831) 459-2935.

(1) (a) Ignarro, L. J. *Nitric Oxide: Biology and Pathobiology*; Academic Press: San Diego, 2000. (b) Nitric Oxide Free Radicals in Peripheral Neurotransmission; Kalsner, S., Ed.; Birkhauser: Boston, 2000. (c) Ko, G. Y.; Fang, F. C. Nitric Oxide and Infection; Kluwer Academic/Plenum Publishers: New York, 1999. (d) Lincoln J.; Burnstock G. Nitric Oxide in Health and Disease; Cambridge University Press: New York, 1997.

(2) (a) Ying, L.; Hofseth, L. J. *Cancer Res.* **2007**, *67*, 1407–1410. (b) Xu, W.; Liu, L. Z.; Loizidou, M.; Ahmed, M.; Charles, I. G. *Cell Res.* **2002**, *12*, 311–320. (c) Fukuto, J. M.; Wink, D. A. *Met. Ions Biol. Syst.* **1999**, *36*, 547–595.

(3) (a) Du, C.; Guan, Q.; Diao, H.; Yin, Z.; Jevnikar, A. M. *Am. J. Physiol.* **2006**, *290*, F1044–F1054. (b) Chung, P.; Cook, T.; Liu, K.; Vodovotz, Y.; Zamora, R.; Finkelstein, S.; Billiar, T.; Blumberg, D. *Nitric Oxide* **2003**, *8*, 119–126. (c) Brüne, B.; Mohr, S. *Curr. Protein Pept. Sci.* **2001**, *2*, 61–72. (d) Chae, H. J.; Chae, S.-W.; An, N.-H.; Kim, J.-H.; Kim, C.-W.; Yoo, S.-K.; Kim, H.-H.; Lee, Z.-L.; Kim, H.-R. *Biol. Pharm. Bull.* **2001**, *24*, 453–460.

(4) (a) Brown, G. C. *Front. Biosci.* **2007**, *12*, 1024–1033. (b) Zhang, J.; Jin, B.; Li, L.; Block, E. R.; Patel, J. M. *Am. J. Physiol. Cell Physiol.* **2005**, *288*, C840–C849. (c) Kadenbach, B.; Arnold, S.; Lee, I.; Hüttermann, M. *Biochim. Biophys. Acta* **2004**, *1655*, 400–408. (d) Boyd, C. S.; Cadenas, E. *Biol. Chem.* **2002**, *383*, 411–423. (e) Brown, G. C. *Biochim. Biophys. Acta* **2001**, *1504*, 46–57.

(5) (a) Mocellin, S.; Bronte, V.; Nitti, D. *Med. Res. Rev.* **2007**, *27*, 317–352. (b) Bobba, A.; Atlante, A.; Moro, L.; Calissano, P.; Marra, E. *Apoptosis* **2007**, *12*, 1597–1610. (c) Tarr, J. M.; Eggleton, P.; Winyard, P. G. *Curr. Pharm. Des.* **2006**, *12*, 4445–4468. (d) Wink, D. A.; Vodovotz, Y.; Laval, J.; Laval, F.; Dewhirst, M. W.; Mitchell, J. B. *Carcinogenesis* **1998**, *19*, 711–721. (e) Dimmeler, S.; Zeihar, A. M. *Nitric Oxide* **1997**, *1*, 275–281.

(6) (a) Hirst, D.; Robson, T. *J. Pharm. Pharmacol.* **2007**, *59*, 3–13. (b) Bonavida, B.; Khineche, S.; Huerta-Yepez, S.; Garbán, H. *Drug Resist. Updates* **2006**, *9*, 157. (c) Li, C. Q.; Wogan, G. N. *Cancer Lett.* **2005**, *226*, 1–15. (d) Hofseth, L. J.; Hussain, S. P.; Wogan, G. N.; Harris, C. C. *Free Radical Biol. Med.* **2003**, *34*, 955–968.

(7) (a) Fukumura, D.; Kashiwagi, S.; Jain, R. K. *Nat. Rev. Cancer* **2006**, *6*, 521–534. (b) Xie, K. P.; Suyun, H. *Free Radical Biol. Med.* **2003**, *34*, 969–986.

Published on Web 05/29/2009

NO donors such as GTN (glyceryl trinitrate), SNAP (*S*-nitrosopenecillamine) and NONOates have been used to induce apoptosis in cancer cell lines.[8−10] However, these systemic NO donors deliver NO via enzymatic and/or pH-dependent pathways and hence are hardly suitable for site-specific NO delivery. One way of providing such delivery of NO to malignant sites would be to employ light-activated NO donors,[11] similar to heme-based photosensitizers (such as Photofrin),[12] used in photodynamic therapy (PDT)[13] for skin malignancies.

Over the past few years, several research groups (including ours) have developed a number of photoactive metal nitrosyls[14] (NO complexes of transition metals[15]) that release NO upon exposure to light. Such complexes have been derived from metals such as iron,[16] manganese,[17] and ruthenium.[18] Some simple iron nitroysls such as Roussin's salt esters $[Fe(NO)_2(SR)_2]$[19] and sodium nitroprusside $Na_2[Fe(NO)(CN)_5]$[20] have been shown to exhibit some photolability of the NO ligand upon exposure to light. We have reported $\{Fe-NO\}^6$ nitrosyls such as $[(PaPy_3)Fe(NO)](ClO_4)_2$ and $[(PaPy_2Q)Fe(NO)](ClO_4)_2$ that rapidly release NO when exposed to visible light of low intensity (mW).[21] Unfortunately, most iron-nitrosyls exhibit poor stability in biological (aqueous) media, and exogenous NO donors like Roussin's salts and $Na_2[Fe(NO)(CN)_5]$ suffer from uncontrolled photodecomposition and toxicity.[22,23] In contrast, $\{Ru-NO\}^6$ nitrosyls are much more stable and release NO in predictable manners under illumination. For example, complexes like $K_2[Ru(NO)(Cl)_5]$[18,24] or $[(PaPy_3)Ru(NO)](BF_4)_2$ have been used in aqueous biological buffers to deliver NO to tissues and proteins.[25] Nitrosyls derived from ligands like H_2Me_2bpb and H_2Me_2bQb (shown below)[26] have also shown to be stable in protic media. The advantages of such ruthenium nitrosyls over other metals (especially Fe) are well-documented.[18] Most of these ruthenium nitrosyls are however *activated only by UV light*, which is a major limitation for use of ruthenium NO donors in biological experiments.

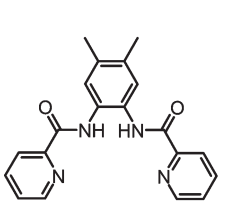

H_2Me_2bpb

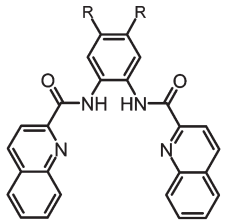

R = Me, H_2Me_2bQb
R = OMe, $H_2(OMe)_2bQb$

In a recent account, we have reported a strategy to overcome this problem of the need of UV light for the activation of typical $\{Ru-NO\}^6$ nitrosyls. Our work has shown that direct ligation of a light-harvesting dye Resorufin (**Resf**, shown below) via the phenolato-O atom to the Ru center of the $\{Ru-NO\}^6$ nitrosyl $[(Me_2bpb)Ru(NO)(Solv)]^+$ sensitizes it to visible light.[27,28] Ford and co-workers have pursued related strategies such as the attachment of various UV chromophores (like pyrene)[29] or visible chromophores (like fluorescein or protoporphyrin IX)[30] via $(CH_2)_n$ linkers to Roussin's salts. Their effort achieved moderate increases in photosensitivity (quantum yield $\phi = 0.025\%$). In contrast, direct coordination of the dye chromophore to the Ru−NO unit allows more effective connectivity between the

(8) Wang P. G.; Cai T. B.; Taniguchi N. *Nitric Oxide Donors for Pharmaceutical and Biological Applications*; Wiley-VCH: Weinheim, 2005.
(9) (a) Degoute, C. S. *Drugs* **2007**, *67*, 1053–1076. (b) Gasco, A.; Fruttero, R.; Rolando, B. *Rev. Med. Chem.* **2005**, *5*, 217–229. Keefer, L. K. *Curr. Topics Med. Chem.* **2005**, *5*, 625–634. (c) Napoli, C.; Ignarro, L. J. *Annu. Rev. Pharmacol. Toxicol.* **2003**, *43*, 97–123. (d) Wang, P. G.; Xian, M.; Tang, X.; Wu, X.; Wen, Z.; Cai, T.; Janczuk, A. J. *Chem. Rev.* **2002**, *102*, 1091–1134. (e) Jia, Q. A.; Janczuk, A. J.; Cai, T. W.; Xian, M.; Wen, Z.; Wang, P. G. *Expert Opin. Ther. Pat.* **2002**, *12*, 819–826.
(10) (a) Velazquez, C. A.; Rao, P.; Citro, M. L.; Keefer, L. K.; Knaus, E. E. *Bioorg. Med. Chem.* **2007**, *15*, 4767–4774. (b) Saavedra, J. E.; Shami, P. J.; Wang, L. Y.; Davies, K. M.; Booth, M. N.; Citro, M. L.; Keefer, L. K. *J. Med. Chem.* **2000**, *43*, 261–269.
(11) (a) Pavlos, C. M.; Xu, H.; Toscano, J. P. *Curr. Top. Med. Chem.* **2005**, *5*, 635–645. (b) Srinivasan, A.; Kebede, N.; Saavedra, J. E.; Nikolaitchik, A. V.; Brady, D. A.; Yourd, E.; Davies, K. M.; Keefer, L. K.; Toscano, J. P. *J. Am. Chem. Soc.* **2001**, *123*, 5465–5472.
(12) (a) Schaffer, M.; Ertl-Wagner, B.; Schaffer, P. M.; Kulka, U.; Jori, G.; Dühmke, E.; Hofstetter, A. *Curr. Med. Chem.* **2005**, *12*, 1209–1215. (b) Brown, S. B.; Brown, E. A.; Walker, I. *Lancet Oncol.* **2004**, *5*, 497–508.
(13) (a) Castano, A. P.; Mroz, P.; Hamblin, M. R. *Nat. Rev. Cancer* **2006**, *6*, 535–545. (b) Detty, M. R.; Gibson, S. L.; Wagner, S. J. *J. Med. Chem.* **2004**, *47*, 3897–3915. (c) Pandey, R. K. *J. Porphyrins Phthalocyanines* **2000**, *4*, 368–373. (d) Stochel, G.; Wanat, A.; Kuliś, E.; Stasicka, Z. *Coord. Chem. Rev.* **1998**, *171*, 203–220.
(14) (a) Rose, M. J.; Mascharak, P. K. *Curr. Opin. Chem. Biol.* **2008**, *12*, 238–244. (b) Ford, P. C.; Bourassa, J.; Miranda, K.; Lee, B.; Lorkovic, I.; Boggs, S.; Kudo, S.; Laverman, L. *Coord. Chem. Rev.* **1998**, *171*, 185–202.
(15) Richter-Addo G. B.; Legzdins P. *Metal nitrosyls*; Oxford University Press: Oxford, U.K., 1992.
(16) (a) Afshar, R. K.; Patra, A. K.; Olmstead, M. M.; Mascharak, P. K. *Inorg. Chem.* **2004**, *43*, 5736–5743. (b) Patra, A. K.; Rowland, J. M.; Marlin, D. S.; Bill, E.; Olmstead, M. M.; Mascharak, P. K. *Inorg. Chem.* **2003**, *42*, 6812–6823. (c) Patra, A. K.; Afshar, R. K.; Olmstead, M. M.; Mascharak, P. K. *Angew. Chem., Int. Ed.* **2002**, *41*, 2512–2515.
(17) (a) Eroy-Reveles, A. A.; Leung, Y.; Beavers, C. M.; Olmstead, M. M.; Mascharak, P. K. *J. Am. Chem. Soc.* **2008**, *130*, 4447–4458. (b) Eroy-Reveles, A. A.; Leung, Y.; Mascharak, P. K. *J. Am. Chem. Soc.* **2006**, *128*, 7166–7167. (c) Ghosh, K.; Eroy-Reveles, A. A.; Avila, B.; Holman, T. R.; Olmstead, M. M.; Mascharak, P. K. *Inorg. Chem.* **2004**, *43*, 2988–2997.
(18) (a) Rose, M. J.; Mascharak, P. K. *Coord. Chem. Rev.* **2008**, *252*, 2093–2114. (b) Rose, M. J.; Patra, A. K.; Alcid, E. A.; Olmstead, M. M.; Mascharak, P. K. *Inorg. Chem.* **2007**, *46*, 2328–2338.
(19) (a) Conrado, C.; Bourassa, J. L.; Egler, C.; Wecksler, S.; Ford, P. C. *Inorg. Chem.* **2003**, *42*, 2288–2293. (b) Bourassa, J. L.; Ford, P. C. *Coord. Chem. Rev.* **2000**, *200−202*, 887–900. (c) Bourassa, J.; DeGraff, W.; Kudo, S.; Wink, D. A.; Mitchell, J. B.; Ford, P. C. *J. Am. Chem. Soc.* **1997**, *119*, 2853–2860.
(20) (a) Singh, R. J.; Hogg, N.; Neese, F.; Joseph, J.; Kalyanaraman, B. *Photochem. Photobiol.* **1995**, *61*, 325–330. (b) Wolfe, S. K.; Swinehart, J. H. *Inorg. Chem.* **1975**, *14*, 1049–1053.
(21) Eroy-Reveles, A. A.; Hoffman-Luca, C. G.; Oliver, A.; Mascharak, P. K. *Dalton Trans.* **2008**, 5268–5274.
(22) (a) Alaniz, C.; Watts, B. *Ann. Pharmacother.* **2005**, *39*, 388–389. (b) Ryu, J.-S.; Lloyd, D. *FEMS Microbiol. Lett.* **1995**, *130*, 183–188.
(23) Janczyk, A.; Wolnicka-Glubisz, A.; Chmura, A.; Elas, M.; Matuszak, Z.; Stochel, G.; Urbanska, K. *Nitric Oxide* **2004**, *10*, 42–50.
(24) (a) Murphy, K.; Williams, J. H.; Bettache, N.; Bliss, T. *Neuropharmacology* **1994**, *33*, 1375–1385. (b) Bettache, N.; Carter, T.; Corrie, J.; Ogden, D.; Trentham, D. R. *Methods Enzymol.* **1996**, *268*, 266–281.
(25) (a) Patra, A. K.; Mascharak, P. K. *Inorg. Chem.* **2003**, *42*, 7363–7365. (b) Szundi, I.; Rose, M. J.; Sen, I.; Eroy-Reveles, A. A.; Mascharak, P. K.; Einarsdóttir, Ó. *Photochem. Photobiol.* **2006**, *82*, 1377–1384. (c) Madhani, M.; Patra, A. K.; Miller, T. W.; Eroy-Reveles, A. A.; Hobbs, A. J.; Fukuto, J. M.; Mascharak, P. K. *J. Med. Chem.* **2006**, *49*, 7325–7330.
(26) Patra, A. K.; Rose, M. J.; Murphy, K. M.; Olmstead, M. M.; Mascharak, P. K. *Inorg. Chem.* **2004**, *43*, 4487–4495.
(27) Rose, M. J.; Olmstead, M. M.; Mascharak, P. K. *J. Am. Chem. Soc.* **2007**, *129*, 5342–5343.
(28) Rose, M. J.; Fry, N. L; Marlow, R.; Hinck, L.; Mascharak, P. K. *J. Am. Chem. Soc.* **2008**, *130*, 8834–8846.
(29) (a) DeRosa, F.; Bu, X.; Pohaku, K.; Ford, P. C. *Inorg. Chem.* **2005**, *44*, 4166–4174. (b) DeRosa, F.; Bu, X.; Ford, P. C. *Inorg. Chem.* **2003**, *42*, 4171–4178.
(30) (a) Wecksler, S. R.; Hutchinson, J.; Ford, P. C. *Inorg. Chem.* **2006**, *45*, 1192–1200. (b) Wecksler, S.; Mikhailovsky, A.; Ford, P. C. *J. Am. Chem. Soc.* **2004**, *125*, 13566–13567.

chromophore and the metal center, and thus greater extent of energy transfer (and sensitization). For example, the dye-sensitized nitrosyl [(Me_2bpb)Ru(NO)(Resf)] exhibits ϕ_{500} (quantum yield of NO photolability at 500 nm) of ~0.05 whereas the dye-free analogue [(Me_2bpb)Ru(NO)(OH)] is *not* photosensitive at this wavelength ($\phi_{500} < 0.001$).[27] It is interesting to note that the intrinsic photoband of the {(Me_2bpb)Ru(NO)} unit is observed at 400 nm, while the absorption of the coordinated dye chromophore($Resf^-$) is centered at 500 nm. We were curious to find out whether this separation is responsible for the moderate degree of enhancement in photosensitization of the parent $\{Ru\text{-}NO\}^6$ nitrosyl in case of [(Me_2bpb)Ru(NO)(Resf)]. Indeed, when the photoband of the {LRu(NO)} unit was systematically red-shifted from 400 to 450 nm to 500 nm by changing the in-plane ligand L from Me_2bpb^{2-} to Me_2bQb^{2-} to $(OMe)_2bQb^{2-}$, the ϕ_{500} value of the resulting nitrosyl-dye conjugates increased from 0.05 to 0.10 to 0.20.[28] It is therefore evident that proper overlap of the photoband of the $\{Ru\text{-}NO\}^6$ nitrosyl with the strong absorption band of the dye (light-harvesting ligand) is critical for sensitization of the nitrosyl-dye conjugates to visible light (Figure 1).

In the present work, we sought to explore the other possibility; instead of altering the in-plane ligand of the $\{Ru\text{-}NO\}^6$ nitrosyl, we have altered the dye ligand. Here we have attached a series of dyes containing different a heteroatom in their tricyclic frame (and hence different λ_{max} of absorption in the visible range) to the same {($(OMe)_2$bQb)Ru(NO)} unit and determined the extent of sensitization of the resulting nitrosyl-dye conjugates to visible light (Figure 1). While selecting the dyes, we have exploited the so-called "heavy-atom" effect mentioned in other PDT studies.[31−33] In case of PDT with singlet oxygen ($^1O_2$), researchers have noted greater sensitization (higher quantum yields) when nitrogen-containing porphyrin sensitizers (such as Photophrin) are substituted with sulfur-, bromine-, or iodine-containing analogues.[32] Such replacements afford approximately 2- to 3-fold increase in ϕ-values. It has been shown that the "heavy-atom" effect arises from increased spin−orbit coupling in larger atoms, which can enhance spin-forbidden transitions.[33] For example, in case of the chalcogenapyrylium dyes, replacement of O centers with S, Se, or Te increases the quantum yields of $^1O_2$ production dramatically.[34] Keeping this in mind,

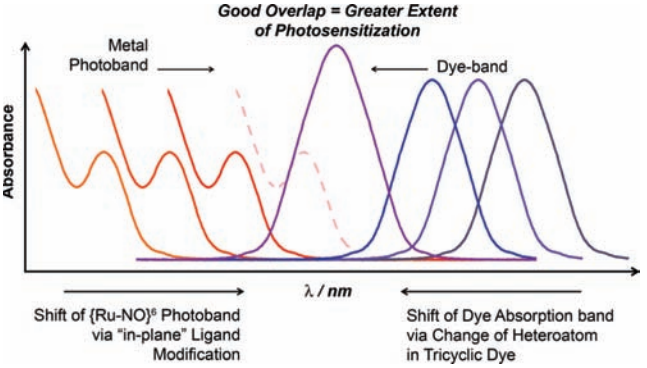

Figure 1. Schematic description of the strategy of merging the photoband of the metal nitrosyl into the strong dye absorption band through direct coordination to the metal center.

we have synthesized a series of iso-electronic heavy-atom (O, S, and Se)[35,36] chromophores based on the heterotricyclic ring system of the phenoxazine dye Resorufin and isolated three nitrosyl-dye conjugates of the general formula [(($(OMe)_2$bQb)Ru(NO)(Dye)] where Dye = deprotonated Resorufin (Resf), Thionol (Thnl), or Selenophore (Seln). In this paper, we report the syntheses of the heavy-atom dye chromophores, as well as the syntheses, structures, spectroscopic

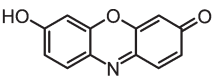

Resorufin

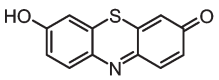

Thionol

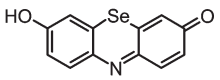

Selenophore

properties, and NO photolabilities of [(($(OMe)_2$bQb)Ru(NO)(Cl)] (**RuNO-Cl**), [(($(OMe)_2$bQb)Ru(NO)(Thnl)] (**RuNO-Thnl**), and [(($(OMe)_2$bQb)Ru(NO)(Seln)] (**RuNO-Seln**). Although the nitrosyl-dye conjugate [(($(OMe)_2$bQb)Ru(NO)(Resf)] (**RuNO-Resf**) has been reported in detail in our previous paper,[28] we have included the corresponding data for this complex in our discussion throughout this paper for the sake of comparison. We also report the results of density functional theory (DFT) calculations on all three nitrosyl-dye conjugates and the parent nitrosyl [(($(OMe)_2$bQb)Ru(NO)(Cl)] (**RuNO-Cl**). The results of such calculations provide insight into the process of energy transfer between the dye chromophores and the {Ru-NO} unit.

Experimental Section

Materials and General Procedures. The ligand $H_2(OMe)_2bQb$ was synthesized from 1,2-dimethoxy-4,5-diaminobenzene, obtained via reduction of 1,2-dimethoxy-4,5-dinitrobenzene (Alfa-Aesar) as previously reported.[37] Commercially available $RuCl_3 \cdot xH_2O$ (Sigma) was used to prepare the $RuCl_3 \cdot 3H_2O$ used in syntheses of ruthenium complexes. NO gas was purchased from

(31) (a) Miskoski, S; Soltermann, A. T.; Molina, P. G.; Günther, G.; Zanocco, A. L.; García, N. A. *Photochem. Photobiol.* **2005**, *81*, 325–332. (b) Gorman, A.; Killoran, J.; O'Shea, C.; Kenna, T.; Gallagher, W. M.; O'Shea, D. F. *J. Am. Chem. Soc.* **2004**, *126*, 10619–10631. (c) Aveline, B. M.; Redmond, R. W. *Photochem. Photobiol.* **1999**, *69*, 306–316.

(32) (a) Serra, A. C.; Pineiro, M.; Rocha Gonsalves, A.; Abrantes, M.; Laranjo, M.; Santos, A. C.; Botelho, M. F. *J. Photochem. Photobiol. B* **2008**, *92*, 59–65. (b) Ha, J.-H.; Kim, M.-S.; Park, Y.-I.; Ryu, S.; Park, M.; Shin, K.; Kim, Y.-R. *Bull. Korean Chem. Soc.* **2002**, *23*, 281–285.

(33) (a) Solovyov, K. N.; Borisevich, E. A. *Phys. Uspekhi.* **2005**, *48*, 231–253. (b) Turro, N. J. *Modern Molecular Photochemistry*; University Science Books: Mill Valley, CA: 1991.(c) Koziar, J. C.; Cowan, D. O. *Acc. Chem. Res.* **1978**, *11*, 334–341. (d) McGlynn, S. P.; Azumi, T.; Kinoshita, M. *Molecular Spectroscopy of the Triplet State*; Prentice Hall: New York, 1969.

(34) (a) Krieg, M.; Bilitz, J. M.; Traul, D. L.; Sieber, F. *Cancer Res.* **1995**, *4*, 163–172. (b) Krieg, M.; Bilitz, J. M.; Srichai, M. B.; Redmond, R. W. *Biochim. Biophys. Acta* **1994**, *1199*, 149–156.

(35) (a) Detty, M. R.; Merkel, P. B.; Hilf, R.; Gibson, S. L.; Powers, S. K. *J. Med. Chem.* **1990**, *33*, 1108–1116. (b) Detty, M. R.; Merkel, P. B. *J. Am. Chem. Soc.* **1990**, *112*, 3845–3855. (c) Powers, S. K.; Walstad, D. L.; Brown, J. T.; Detty, M.; Watkins, P. J. *J. Neuro-Oncology* **1989**, *7*, 179–188. (d) Detty, M. R.; Merkel, P. B. *J. Am. Chem. Soc.* **1988**, *110*, 5920–5922.

(36) (a) Detty, M. R.; O'Regan, M. B. *Heterocyclic Compounds: Tellurium-Containing Heterocycles*; Wiley-Interscience: New York, 1994. (b) Organic Selenium Compounds: Their Chemistry and Biology; Klayman, D. L.; Gunther, W. H. H, Eds.; Wiley-Interscience: New York, 1973.

(37) Rosa, D. T.; Reynolds, R. A.; Malinak, S. M.; Coucouvanis, D. *Inorg. Synth.* **2002**, *33*, 112–119.

Spectra Gases, Inc. and purified as previously described.[26] Solvents were purchased from Fisher Scientific and distilled according to standard procedures: Et_2O and THF from Na; CH_2Cl_2 and MeCN from CaH_2; $CHCl_3$ from K_2CO_3; DMF from BaO; pentane was used without further purification. $AgBF_4$ was obtained from Alfa-Aesar, while selenium chloride (Se_2Cl_2) was purchased from Strem Chemicals. Resorufin (as Na salt), phenothiazine and diphenylamine were procured from Sigma-Aldrich.

[((OMe)$_2$bQb)Ru(NO)(Cl)] (RuNO-Cl). This nitrosyl was synthesized by following the procedure previously reported by us. Crystals of **RuNO-Cl·CHCl$_3$**, suitable for diffraction study, were grown via vapor diffusion of pentane into a $CHCl_3$ solution of the complex. UV/vis in $CHCl_3$ (for comparisons in this study), λ in nm (ε in M^{-1} cm^{-1}): 500 (4950), 323 (26900).

Li Salt of Thionol, 7-Hydroxy-phenothiazin-3-one (Li-Thnl). This dye was synthesized by following a published procedure,[38] with some modifications. A batch of phenothiazine (5 g, 25.1 mmol) was oxidized in 120 mL of a 5:1 mixture of conc. H_2SO_4: H_2O by heating to 165 °C for 12 h. The dark red solution was cooled to room temperature and poured into 250 mL of H_2O to generate a blackish-purple solid, which was collected by filtration and washed with 2 × 30 mL of H_2O. This crude solid was then extracted briefly with a boiling solution of aqueous Na_2CO_3 (2 g in 250 mL), and the pale red filtrate was discarded. Next, the crude solid was extracted a second time with boiling aqueous Na_2CO_3 (2 g in 250 mL) for an extended period (15 min). The dark violet filtrate was placed at 4 °C overnight to precipitate trace impurities. Next, 6 g of LiCl was added, and the mixture was stored at 4 °C for several days to obtain pure Li-Thnl as dark violet crystalline material. Yield: 600 mg (13%). Anal. cacld. for $C_{12}H_6NO_2SLi$ (Thnl-Li): C 61.28, H 2.57, N 5.96; found: C 61.09, H 2.75, N 6.01. Selected IR bands (KBr matrix, cm^{-1}): 1581 (s ν_{CO}), 1499 (m), 1466 (m), 1381 (s), 1313 (s), 1300 (m), 1214 (m), 1118 (w), 854 (s), 765 (w), 538 (m). UV/vis in DMF, λ in nm (ε in M^{-1} cm^{-1}): 328 (11 460), 567 (25 790), 610 (91 260). UV/vis in DMF/AcOH (1:1), λ in nm (ε in M^{-1} cm^{-1}): 422 (10 090), 507 (13 460). ^{1}H NMR in $(CD_3)_2SO$, δ from TMS: 7.34 (s 1H), 7.33 (s 1H), 6.38 (d 1H), 6.36 (d 1H), 6.28 (m 2H). ESI-MS: m/z 229.87 (Thnl-H due to 0.1% TFA).

[((OMe)$_2$bQb)Ru(NO)(Thnl)] (RuNO-Thnl). A batch of **RuNO-Cl** (0.110 g, 0.162 mmol) was slurried in 20 mL of a 1:1 mixture of MeCN/THF in presence of 1 equiv of $AgBF_4$ (32 mg, 0.162 mmol) and heated to reflux temperature for 4 h. The turbid red solution thus obtained was filtered at room temperature (to remove AgCl), and 1 equiv of Li-Thnl dye was added to the filtrate. The mixture was again heated to reflux for 6 h when a bright red solution was obtained. Next, the solution was hot-filtered (to remove trace amount of unreacted dye), and the solvent was removed in vacuo. The dark red residue was then dissolved in $CHCl_3$ and purified by silica gel chromatography using a CH_2Cl_2/THF gradient. Finally, the complex was isolated by diffusing Et_2O vapor into the concentrated eluate. Yield: 45 mg (34%). Anal. Calcd for $C_{40}H_{26}N_6O_7SRu$ (**RuNO-Thnl**): C 57.48, H 3.14, N 10.06; found: C 57.55, H 3.08, N 10.16. X-ray quality crystals of **RuNO-Thnl** were obtained via vapor diffusion of pentane into a $CHCl_3$ solution of the complex. Selected IR bands (KBr matrix, cm^{-1}): 1847 (s ν_{NO}), 1618 (vs ν_{CO}), 1589 (vs ν_{CN}), 1511 (w), 1494 (w), 1469 (m), 1340 (w), 1270 (m), 1211 (m), 1101 (w), 1078 (w), 870 (w). UV/vis in $CHCl_3$, λ in nm (ε in M^{-1} cm^{-1}): 525 (24 930), 445 (16 220), 318 (27 000). ^{1}H NMR in $CDCl_3$, δ from TMS: 8.74 (d 2H), 8.49 (d 2H), 8.35 (s 2H), 8.16 (d 2H), 8.14 (d 2H), 7.81 (t 2H), 7.56 (t 2H), 7.46 (t 2H), 7.23 (d 1H), 7.09 (s 1H), 6.80 (d 1H), 6.57 (s 1H), 5.99 (d 1H), 5.91 (s 1H). ESI-MS: m/z 835.86.

Selenophore, 7-Hydroxy-phenoselenazin-3-one (Seln). A solution of Se_2Cl_2 (1.47 g, 6.44 mmol) in 10 mL of toluene was slowly added to a solution of 2.18 g (12.88 mmol) of diphenylamine in 50 mL of toluene when a dark brown precipitate was observed. Next, the mixture was heated to reflux for 4 h to generate an turbid orange solution. The solution was filtered, and toluene was removed from the filtrate in vacuo, leaving a pumpkin-orange colored crude batch of phenoselenozine. This solid was then subjected to the oxygenating conditions used above for phenothiazine (35 mL of H_2SO_4/H_2O 4:1 mixture at 165 °C), except for much shorter heating times (only 1 h for phenoselenozine versus 12 h for phenothiazine). The resulting deep red solution was diluted with an equal volume of H_2O, and the crude precipitate was collected on a Buchner funnel. This solid was first washed with 3 × 20 mL of boiling H_2O containing of 0.5 g of Na_2CO_3, and each time the red filtrate was discarded. The residue was then extracted with 3 × 20 mL of boiling Na_2CO_3 solution. The extracts were pooled, and the intensely bluish-violet solution was slowly neutralized with 20 mL of AcOH to generate a reddish solution at pH 5. Next, the solvent(s) was removed, and the residue was dissolved in CH_2Cl_2 containing 1% AcOH and loaded onto a silica gel column equilibrated with the same solution. A bright red band was eluted with a CH_2Cl_2/THF/MeOH gradient. Removal of the solvent afforded a red oil. Redissolving this oil in minimum amount (~0.5 mL) of CH_2Cl_2/THF followed by stirring afforded pure Seln as a violet solid. Yield: 240 mg (12%). Anal. Calcd for $C_{12}H_7NO_2Se$ (Seln): C 52.19, H 2.55, N 5.07; found: C 52.08, H 2.43, N 4.98. X-ray quality crystals (violet blocks) of Seln were grown by Et_2O vapor diffusion into a CH_2Cl_2/THF solution (containing 1% AcOH) of the dye. Selected IR bands (KBr matrix, cm^{-1}): 2963 (w), 1597 (m), 1435 (m), 1290 (w), 1261 (s), 1210 (m), 865 (w), 800 (s). UV/vis in DMF as Na salt, λ in nm (ε in M^{-1} cm^{-1}): 612 (80 000). UV/vis in DMF/AcOH (1:1), λ in nm (ε in M^{-1} cm^{-1}): 428 (10 070), 513 (9 720). ESI-MS: m/z 277.86 and 275.87.

[((OMe)$_2$bQb)Ru(NO)(Seln)] (RuNO-Seln). A batch of 50 mg (0.078 mmol) of **RuNO-Cl** was treated with $AgBF_4$ in boiling MeCN and later filtered as described for **RuNO-Thnl**. Next, a blue slurry of the selenophore dye (22 mg, 0.078 mmol) and 1 equiv of NaH (2 mg) in 10 mL of MeCN were added to the filtrate, and the mixture heated to reflux for 3 h. It was then hot-filtered to remove unreacted dye and $NaBF_4$. The solvent was removed in vacuo, and the residue was purified by silica column chromatography as described for **RuNO-Thnl**. Yield: 20 mg (30%). Anal. Calcd for $C_{40}H_{26}N_6O_7SeRu$ (**RuNO-Seln**): C 54.43, H 2.97, N 9.52; found: C 54.47, H 3.04, N 9.48. X-ray quality crystals of **RuNO-Seln** (long parallelepipeds) were obtained by vapor diffusion of Et_2O into a CH_2Cl_2/THF (1:1) mixture. Selected IR bands (KBr matrix, cm^{-1}): 1847 (s ν_{NO}), 1616 (vs ν_{CO}), 1588 (s ν_{CN}), 1512 (w), 1496 (m), 1466 (m), 1340 (w), 1270 (m), 1211 (s), 1100 (w), 864 (m), 763 (m). UV/vis in $CHCl_3$, λ in nm (ε in M^{-1} cm^{-1}): 535 (22 330), 455 (17 380), 320 (25 010). ESI-MS: m/z 884.78 and 886.75.

X-ray Diffraction, Data Collection, and Structure Solution. Diffraction data for the free dye Seln and **RuNO-Cl·CHCl$_3$** (153 K) were collected on a Bruker Apex-II diffractometer with Mo Kα radiation (λ = 0.71073 Å). The data for **RuNO-Thnl·0.5CH$_2$Cl$_2$·H$_2$O** and **RuNO-Seln** (150 K) were collected using synchrotron radiation (λ = 0.77490 Å) at the Lawrence-Berkeley Advanced Light Source (ALS). All data were processed and structures solved using the SHELXTL software package. Crystal properties, diffraction data, and parameters for structure solution are listed in Table 1 while selected bond distances (Å) and bond angles (deg) are included in Table 2.

Physical Measurements. ^{1}H NMR spectra were obtained with a Varian 500 MHz spectrometer. A Cary 50 scanning spectrophotometer (Varian) was used to record the electronic absorption spectra of the nitrosyl-dye conjugates. Because of solubility and stability concerns, most of the absorption measurements on the nitrosyl-dye conjugates were performed in $CHCl_3$ or MeCN.

(38) Granick, S.; Michaelis, L. *J. Am. Chem. Soc.* **1947**, *69*, 2983–2986.

Solid-state IR spectra (KBr disk) of the chromophores and nitrosyls were recorded on a Perkin-Elmer Spectrum One FTIR spectrometer. Mass spectral data were acquired using a Micromass ZMD electrospray spectrometer. X-band EPR spectra were obtained using a Bruker 500 ELEXSYS spectrometer (125 K) while the fluorescence (298 K) or phosphorescence (77 K) emission spectra were recorded with a Perkin-Elmer LS-50B Fluorescence/Luminescence Spectrometer. Photorelease of NO in aqueous solution was detected with *in*NO Nitric Oxide Monitoring System (Innovative Instruments, Inc.) fitted with an *ami*-NO-2000 electrode.

Photolysis Experiments. Samples of the nitrosyls were prepared in 4 × 10 mm quartz cuvettes and placed 2 cm from the light source. Solutions were prepared at ~0.2 mM to ensure sufficient absorbance (>90%) at the irradiation wavelength, and changes in electronic spectra in the 750 nm region (<10% photolysis) were used to determine the apparent rates of NO photorelease. Actinochrome N (475/610) was used as the quantum yield (ϕ) standard in the visible range. The rates of NO photorelease were determined with the aid of monochromatic light from a tunable Apex Illuminator (150 W xenon lamp) equipped with a Cornerstone 130 1/8 M monochromator (measured intensity of ~10 mW). For determination of the $\phi_{500-600}$ values, an IL 410 Illumination System (Electro-FiberOptics Corp.) equipped with $\lambda \geq 465-600$ nm cutoff filters (measured intensity of outcoming light = 200−300 mW) was used. The same system was employed for qualitative EPR measurements on the photoproducts. In such experiments, solutions were

Table 1. Summary of Crystal Data, Intensity Collection, and Refinement Parameters for [((OMe)$_2$bQb)Ru(NO)(Cl)]·$CHCl_3$ (**RuNO-Cl**·$CHCl_3$), [((OMe)$_2$bQb)Ru(NO)(Resf)] (**RuNO-Resf**), [((OMe)$_2$bQb)Ru(NO)(Thnl)]·H_2O·0.5CH_2Cl_2 (**RuNO-Thnl**·H_2O·0.5CH_2Cl_2), [((OMe)$_2$bQb)Ru(NO)(Seln)] (**RuNO-Seln**), and the Free Dye Selenophore

	RuNO-Cl	**RuNO-Thnl**	**RuNO-Seln**	selenophore
empirical formula	$C_{27}H_{23}N_5O_3Cl_4Ru$	$C_{40.5}H_{29}N_6O_8Cl\ S\ Ru$	$C_{40}H_{26}N_6O_8Se\ Ru$	$C_{12}H_6N\ O_2Se$
Fw	708.37	896.28	882.70	275.14
crystal color and habit	orange plates	violet needle	red block	red block
crystal size (mm)	0.27 × 0.18 × 0.04	0.10 × 0.07 × 0.04	0.11 × 0.09 × 0.08	0.10 × 0.10 × 0.08
T (*K*)	153(2)	150(2)	150(2)	153(2)
wavelength (Å)	0.71073	0.7749	0.7749	0.71073
crystal system	monoclinic	monoclinic	monoclinic	triclinic
space group	$P2_1/c$	$P2_1/c$	$P2_1/c$	$P\bar{1}$
a (Å)	10.3596(8)	11.587(2)	10.7125(9)	7.4489(12)
b (Å)	28.611(2)	20.549(4)	20.9291(18)	10.9453(17)
c (Å)	10.1347(7)	15.567(3)	15.3893(13)	12.295(2)
α (deg)	90	90	90	103.180(2)
β (deg)	112.4500(10)	91.68(3)	97.6600(10)	96.138(2)
γ (deg)	90	90	90	96.173(2)
V (Å^3)	2776.3(4)	3705.0(13)	3419.5(5)	961.4(3)
Z	4	4	4	2
d_{calc} (g/cm^3)	1.695	1.607	1.715	1.901
μ (mm^{-1})	0.990	0.767	1.969	3.885
GOF on F^2	1.026	1.132	1.053	0.803
final *R* indices	*R1* = 0.0307	*R1* = 0.0545	*R1* = 0.0411	*R1* = 0.0293
[$I > 2\sigma(I)$]	w*R2* = 0.0690	w*R2* = 0.1530	w*R2* = 0.1196	w*R2* = 0.0946
R indices	*R1* = 0.0414	*R1* = 0.0596	*R1* = 0.0459	*R1* = 0.0372
all data	w*R2* = 0.0738	w*R2* = 0.1567	w*R2* = 0.1236	w*R2* = 0.1023

Table 2. Selected Bond Distances (Å) and Bond Angles (deg) for **RuNO-Cl**, **RuNO-Resf**, **RuNO-Thnl**, **RuNO-Seln**, and Unbound Selenophore along with the Optimized DFT Bond Distances and Bond Angles for Comparison

	RuNO-Cl		RuNO-Resf(O)		RuNO-Thnl(S)		RuNO-Seln(Se)		selenophore
	X-ray	DFT	X-ray	DFT	X-ray	DFT	X-ray	DFT	X-ray
				Bond Distances					
Ru−N5	1.7457(18)	1.743	1.7425(19)	1.736	1.735(3)	1.735	1.739(2)	1.738	
N5−O3	1.148(2)	1.162	1.154(2)	1.163	1.151(4)	1.162	1.155(3)	1.161	
Ru−N1	2.1877(18)	2.184	2.1516(18)	2.192[a]	2.181(3)	2.227[a]	2.158(2)	2.192[a]	
Ru−N2	1.9972(19)	1.992	1.9840(19)	1.983	1.984(3)	1.984	1.980(2)	1.982	
Ru−N3	1.9971(18)	1.989	1.9943(18)	1.996	2.005(3)	1.996	1.997(2)	1.995	
Ru−N4	2.1536(18)	2.189[a]	2.1457(19)	2.186[a]	2.175(3)	2.197	2.181(2)	2.199	
Ru−Cl	2.3754(6)	2.365							
Ru−O(Resf)			1.9915(16)	2.013	2.010(3)	2.025	2.0081(18)	2.019	
O_{ph}−C(Resf)			1.323(3)	1.328	1.319(4)	1.326	1.328(3)	1.329	1.3005(37)
O_{ket}−C(Resf)			1.232(3)	1.234	1.256(5)	1.234	1.243(4)	1.234	1.2929(37)
C−Y (Y = O, S, Se)			1.377(3)	1.365	1.738(4)	1.754	1.871(3)	1.885	1.8779(28)
C−Y (Y = O, S, Se)			1.368(3)	1.363	1.729(4)	1.750	1.881(2)	1.888	1.8784(29)
				Bond Angles					
Ru−N5−O3	175.73(19)	172.09	174.48(19)	178.46	177.1(3)	176.21	176.6(2)	177.89	
Ru−O−C(Resf)			131.80(14)	131.83	133.4(2)	132.40	132.71(16)	132.65	
C−Y−C (Y = O, S, Se)			118.50(19)	119.38	103.03(18)	102.89	99.32(11)	99.62	98.72(13)

[a] Deviations of ~0.04 Å were observed in the Ru−N(Quinolone) bond distances presumably because DFT/B3PW91 slightly overestimates the steric/twisting effect.

photolyzed in quartz cuvettes and transferred to EPR tubes for spectral analyses.

DFT Calculations. DFT calculations were carried out using the double-ζ basis set 6-31G* for all atoms except Ru, for which the quasi-relativistic Stuttgart-Dresden effective core potential (ECP) was implemented. The 6-311G* basis set was used for Se in **RuNO-Seln**. Calculations were carried out with the aid of the program PC-GAMESS[39] using the hybrid functional B3PW91, which (along with Stuttgart Ru-ECP) has been shown to be accurate for second-row transition metals,[40] as well as group 8 elements.[41] The X-ray coordinates of **RuNO-Cl**, **RuNO-Resf**, **RuNO-Thnl**, and **RuNO-Seln** were used as starting point for each geometry optimization and molecular orbital (MO) energy level analysis. MOs were visualized in MacMolPlt for analysis.[42]

Results and Discussion

As mentioned above, the major goal of this study was to start with the {$(OMe)_2$bQb)Ru(NO)} moiety (λ_{max} of the photoband at 500 nm), directly attach a set of isoelectronic tricyclic dyes with different heteroatoms (hence different absorption maxima) to the Ru center, and determine the extent of photosensitization at longer wavelengths of light. On the basis of empirical data in the case of other chromophores,[34] we anticipated that (a) insertion of heavier atoms in the dye chromophores would red-shift the dye bands,[43] (b) promote photoexcitation of the nitrosyl-dye conjugates under lights of *longer* wavelengths, and (c) also enhance the overall efficiency (quantum yield, ϕ) of NO photolability in the visible range because of the heavy-atom effect.[33]

The parent nitrosyl [$((OMe)_2$bQb)Ru(NO)(Cl)] (**RuNO-Cl**) has been synthesized from $(OMe)_2bQb^{2-}$, $RuCl_3$, and NO(g) in DMF by following the published procedure.[28] Removal of the chloride ligand with $AgBF_4$ in MeCN followed by heating of the solvate intermediate with deprotonated dyes afforded the nitrosyl-dye conjugates [$((OMe)_2$bQb)Ru(NO)(Resf)] (**RuNO-Resf**), [$((OMe)_2$bQb)-Ru(NO)(Thnl)] (**RuNO-Thnl**), and [$((OMe)_2$bQb)Ru(NO)-(Seln)] (**RuNO-Seln**) in moderate yields (Scheme 1). The first nitrosyl-dye conjugate, **RuNO-Resf**, has already been reported in a previous account.[28]

Out of the three dyes, only Resf is commercially available. Extension of our synthetic strategy to attach isoelectronic dyes with heavy-atoms therefore required syntheses of the two congeners, Thionol (Y = S, Scheme 1) and Selenophore (Y = Se, Scheme 1) in the present work. Oxygenation of phenothiazine (Y = S) with a mild oxygenating agent (H_2SO_4) at elevated temperatures (165 °C), followed by neutralization with Na_2CO_3 and selective crystallization of the dye as Li salt (with excess LiCl) provided analytically pure Thionol (Thnl).[38] Although our initial reactions of Li-Thnl with the {$(OMe)_2$bQb)Ru(NO)} moiety in refluxing MeCN were unsuccessful (possibly because of the high affinity of Li^+ for the phenolato-O center of the dye), simple change of solvent to MeCN/THF mixture allowed isolation of the dye-nitrosyl conjugate (Scheme 2). This is most likely due to better solvation of Li^+ as a leaving group in THF solution.

Scheme 1

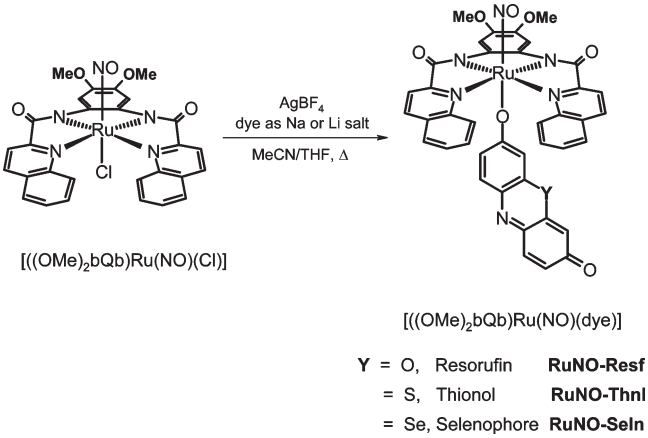

The selenium-containing dye Selenophore (Y = Se, Seln) was synthesized from the selenium congener of phenothiazine, namely, phenoselenazine, obtained from reaction of diphenylamine with Se_2Cl_2 in boiling toluene (Scheme 3).[44] The triheterocycle was then oxygenated with H_2SO_4 at high temperature (165 °C). The best yields were obtained at much shorter reaction times (1 h for Seln versus 12 h for Thnl) indicating higher reactivity of Seln. We were unable to selectively precipitate this dye as its Li (or Na, K) salt. However, column chromatography afforded pure acidic (phenol OH) form of the dye in moderate yield. In this work, we have also determined the structure of the product Seln by crystallography (Figure S1, Supporting Information) to confirm the regioselective insertion of the Se-atom in the tricyclic framework. Reaction of the deprotonated (with NaH) Seln dye with the {$(OMe_2$bQb)Ru(NO)} moiety in refluxing MeCN afforded the desired nitrosyl-dye conjugate [$((OMe)_2$bQb)Ru(NO)(Seln)] (**RuNO-Seln**). We found that it was *essential to maintain total dark conditions* during the syntheses, column purification, and crystallization of **RuNO-Seln**. In contrast, **RuNO-Cl**, **RuNO-Resf**, and **RuNO-Thnl** were somewhat tolerant of ambient light. This was an early indication of the higher extent of photosensitization in case of **RuNO-Seln** (vide infra).

The three nitrosyl-dye conjugates, **RuNO-Resf**, **RuNO-Thnl**, and **RuNO-Seln** exhibit limited solubility in water although they dissolve readily in MeCN and $CHCl_3$. Out of the three, **RuNO-Resf** is the most stable in aqueous solution. However, the dye slowly dissociates over the course of several hours in aqueous solution (pH 5−7). Interestingly, **RuNO-Resf** is less stable in water compared to its congener [$(Me_2$bpb)Ru(NO)(Resf)],[28] presumably because of steric interactions between the quinoline moieties and the bound dye (Figure 3). In case of **RuNO-Thnl**

(39) Nemukhin, A. V.; Grigorenko, B. L.; Granovsky, A. A. *Moscow Univ. Chem. Bull.* **2004**, *45*, 75.
(40) Waller, M. P.; Braun, H.; Hojdis, N.; Bühl, M. *J. Chem. Theory Comput.* **2007**, *3*, 2234–2242.
(41) Hirva, P.; Haukka, M.; Jakonen, M. *J. Mol. Modell.* **2008**, *14*, 171–181.
(42) Bode, B. M.; Gordon, M. S. MacMolPlt: A Graphical User Interface for GAMESS. *J. Mol. Graphics Modell.* **1998**, *16*, 133-138.
(43) (a) Griffiths, J. *Colour and Constitution of Organic Molecules*; Academic Press: London, 1976. (b) Fabian, J.; Hartmann, H. Light Absorption of Organic Colorants; Springer-Verlag: Berlin, 1980. (c) Zollinger, H. Color Chemistry: Syntheses, Properties, and Applications of Organic Dyes and Pigments; Wiley-VCH: Zürich, 2003.
(44) (a) Showalter, H. D.; Sercel, A. D.; Leja, B. M.; Wolfangel, C. D.; Ambroso, L. A.; Elliott, W. L.; Fry, D. W.; Kraker, A. J.; Howard, C. T.; Lu, G. H.; Moore, C. W.; Nelson, J. M.; Roberts, B. J.; Vincent, P. W.; Denny, W. A.; Thompson, A. M. *J. Med. Chem.* **1997**, *40*, 413–426. (b) Behrens, J.; Hinrichs, W.; Link, T.; Schiffling, C.; Klar, G. *Phosphorus, Sulfur Silicon Relat. Elem.* **1995**, *101*, 235–244.

Scheme 2. Synthesis of Thionol (Thnl) from Phenothiazine

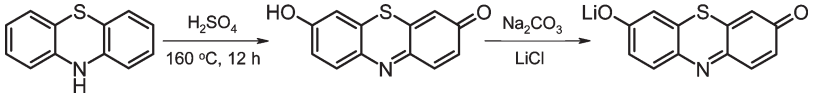

Scheme 3. Synthesis of Selenophore (Seln) from Diphenylamine and Selenium Chloride

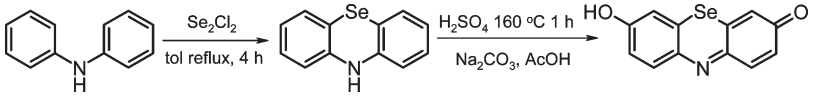

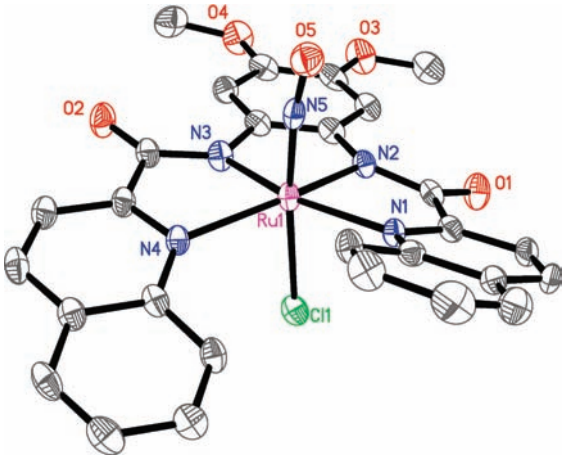

Figure 2. Thermal ellipsoid plot (shown as 50% probability ellipsoids) of [((OMe)$_2$bQb)Ru(NO)(Cl)] (**RuNO-Cl**). H atoms have been omitted for the sake of clarity.

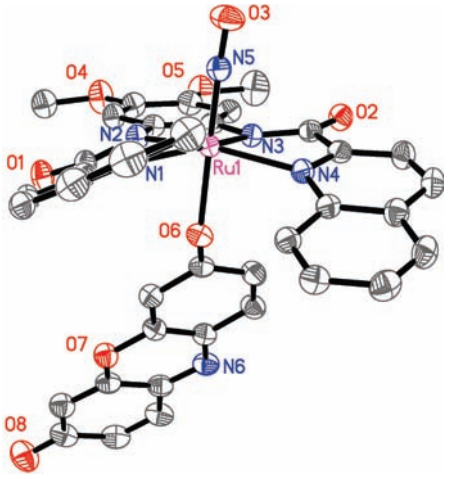

Figure 3. Thermal ellipsoid plot (shown as 50% probability ellipsoids) of [((OMe)$_2$bQb)Ru(NO)(Resf)] (**RuNO-Resf**). H atoms have been omitted for the sake of clarity.

and **RuNO-Seln**, the dye dissociates faster in aqueous solution (within 1 h). For these reasons, the spectral measurements have been performed mostly in $CHCl_3$.

Structures. RuNO-Cl. The structural features of the {(OMe)$_2$bQb)Ru(NO)} moiety in this nitrosyl resemble those of the same unit present in **RuNO-Resf** and the other two nitrosyls reported in this paper (Table 2). As shown in Figure 2, the pseudo-octahedral Ru center is coordinated by the dianionic, dicarboxamido (OMe)$_2$bQb^{2-} ligand in the equatorial plane. Close examination of Table 2 reveals a narrow range of Ru−N_{amido} (1.9840(19) to 2.005(3) Å) and Ru−$N_{quinoline}$ (2.1457(19) to 2.1877(18) Å) distances in all four nitrosyls. Within the {Ru-NO}^{6} unit, both the Ru−N bond distances (1.735(3) to 1.7457(18) Å) and the N−O bond distances (1.148(2) to 1.154(2) Å) are typical for {Ru-NO}^{6} nitrosyls derived from anionic ligands.[18,45] For example, the salen complex [(salen)Ru(NO)(Cl)] exhibits Ru−N distance of 1.7286(6) Å, and a N−O bond distance of 1.149(7) Å.

Steric interactions between the extended quinoline moieties in the equatorial plane of **RuNO-Cl** results in significant twisting of the (OMe)$_2$bQb^{2-} ligand frame.[26,28] This twist of approximately 35° is also observed in **RuNO-Resf** (Figure 3), **RuNO-Thnl** (Figure 4), and **RuNO-Seln** (Figure 5). The presence of the twisted ligand frame in **RuNO-Cl** clearly suggests that the twist observed in the

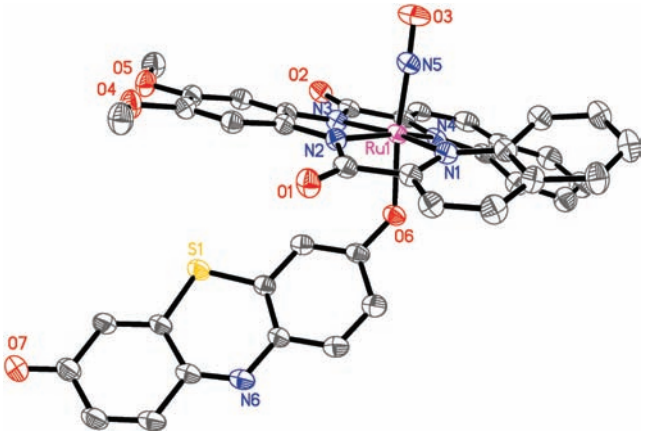

Figure 4. Thermal ellipsoid plot (shown as 50% probability ellipsoids) of [((OMe)$_2$bQb)Ru(NO)(Thnl)] (**RuNO-Thnl**). H atoms have been omitted for the sake of clarity.

three nitrosyl-dye conjugates does not arise from coordination of the bulky dye molecules in axial position but rather is an inherent property of the {(OMe)$_2$bQb)Ru-(NO)} moiety.

RuNO-Resf, RuNO-Thnl, and RuNO-Seln. Since the structural features of the three nitrosyl-dye conjugates are similar to each other, we discuss them as a group. Although the structure of **RuNO-Resf** has been reported in our earlier account,[28] we have included the structure in Figure 3 for the sake of comparison. The structures shown in Figures 3, 4, and 5 confirm direct ligation of the dyes to the Ru centers via the phenolato-O atom. As discussed later, this direct binding facilitates a continuity

(45) (a) Bordini, J.; Hughes, D. L.; Da Motta Neto, J. D.; da Cunha, J. C. *Inorg. Chem.* **2002**, *41*, 5410–5416. (b) Sellmann, D.; Häußinger, D.; Gottschalk-Gaudig, T.; Heinemann, F. W. *Z. Naturforsch.* **2000**, *55b*, 723–729.

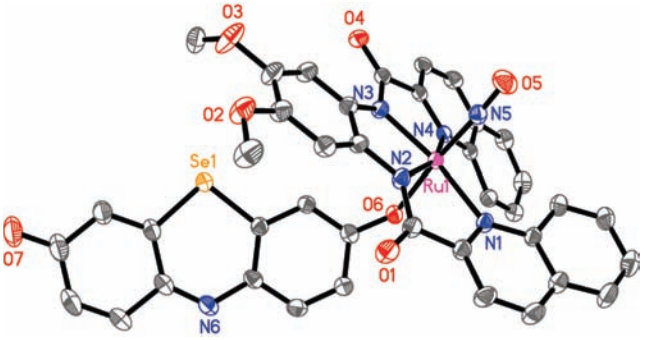

Figure 5. ORTEP diagram of the X-ray structure of [((OMe)$_2$bQb)Ru(NO)(Seln)] (**RuNO-Seln**) shown at 50% thermal ellipsoids, with H atoms omitted for clarity.

of conjugation throughout the π-system of the dye all the way to the bound NO via the d_π orbitals of the metal center—a feature that is crucial for through-bond (Dexter) energy transfer.[33] The Ru−O bond distances lie within a narrow range (1.9915(16) to 2.010(3) Å), a fact that indicates similar bonding between the phenolato-O atom of the dye and the Ru center in all three cases. Notably, these bond distances are much shorter than the Ru−Cl bond distance (2.3754(6) Å) observed in **RuNO-Cl**. In all three structures, the Resf, Thnl, or Seln dye stay tilted away from the O−Ru−NO axis by ~135°, albeit in slightly different directions.

The structural features of the dye chromophores, themselves, warrant some discussion at this point since they display the effects of heavy-atom substitution in the central ring of the tricyclic system. The larger size of the S or Se atoms induces a "prying open" deformation in the central ring of the dye unit (Figures 4 and 5). For example, the average C−Y (Y = O, S, Se) bond distance steadily increases from 1.377(3) to 1.738(4) to 1.881(2) Å as one moves from Resf(O) to Thnl(S) to Seln(Se) and correspondingly, the C−Y−C bond angle becomes more acute (118.50(19) > 103.03(18) > 99.32(11)°). Also, some of the internal angles of the central ring diverge from their ideal value of 60° as one goes from O to S to Se, presumably because of increasing size of the heavy atom. The other structural features of the dyes such as the phenolato C−O bonds (1.319(4) to 1.323(3) Å) and C=O bonds (1.232(3) to 1.256(5) Å) remain relatively unchanged (Table 2).

Electronic Absorption Spectra. Before we examined the electronic absorption features of the nitrosyl-dye conjugates, we investigated the absorption characteristics of the free dye molecules and the parent nitrosyl **RuNO-Cl** separately. This was necessary since we intended to eventually gain insight into how the two chromophores (the dye and the nitrosyl) interact with each other.

Resorufin (Resf), Thionol (Thnl), and Selenophore (Seln). The deprotonated form of each dye (Na or Li salt) exhibits one strong absorption band in the ~600 nm region, with some notable differences. For example, in DMF Resf$^-$ exhibits its intense absorption band

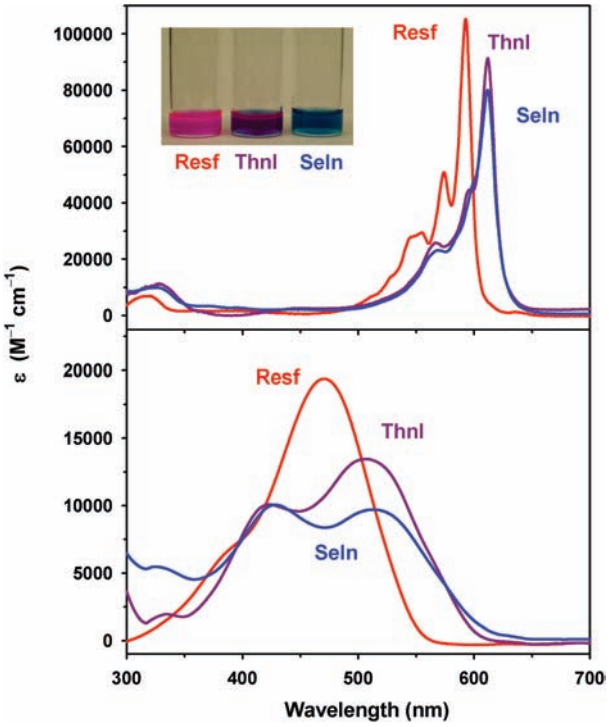

Figure 6. Electronic absorption spectra of Resf, Thnl, and Seln in deprotonated (in DMF, top panel) and protonated (in DMF/AcOH, bottom panel) forms. Inset: Picture of each deprotonated dye in DMF.

(ε = 105 000 M^{-1} cm^{-1}) with λ_{max} at 590 nm (Figure 6, top panel). This band, arising from a highly favored $\pi \rightarrow \pi^*$ transition,[46] appears at low energy because of extensive delocalization of the negative charge of the phenolato-O moiety over the entire tricyclic ring system. Thnl$^-$ exhibits a similar but red-shifted absorption feature centered at 610 nm (Figure 6). The intensity of this band is slightly lower (ε = 91 300 M^{-1} cm^{-1}) than that of Resf$^-$. This trend continues in case of the Se-containing dye Seln$^-$ which exhibits its absorption band at 612 nm with decreased ε-value (80 000 M^{-1} cm^{-1}).[38] Although the absorption parameters for Thnl$^-$ and Seln$^-$ are not significantly different, the colors of their solutions tell a different story (Figure 6, top panel inset). A clear change of color is observed from reddish-violet (Resf$^-$), to bluish-violet (Thnl$^-$), to the pure blue color of Seln$^-$. It is evident that changes in the heteroatom from O to S to Se results in red-shift of the absorption bands of the dyes, a trend that supports our photosensitization strategy.

Dramatic changes in the absorption spectra are observed when the dyes are protonated. In acidic solutions (DMF/AcOH), all three dyes exhibit changes in absorption parameters in terms of λ_{max}, ε-value, as well as half-height width (Figure 6, bottom panel). For example, the λ_{max} of Resf is blue-shifted by 120 nm, down to 470 nm. Additionally, the intensity of the band is decreased by more than 5-fold (ε = 20 000 M^{-1} cm^{-1}). Similar decrease in ε-value is observed in case of Thnl (ε = 13 500 M^{-1} cm^{-1}) and Seln (ε = 9 800 M^{-1} cm^{-1}). Also, the λ_{max} values move to higher energy region (Figure 6, bottom panel). Interestingly, for all three dyes, the absorption bands become broad compared to the extremely sharp features of the dyes in basic forms (Figure 6, top panel). Very similar changes in the absorption features of the dyes are

(46) (a) Montejano, H. A.; Gervaldo, M.; Bertolotti, S. G. *Dyes Pigm.* **2005**, *64*, 117–124. (b) Bueno, C.; Villegas, M. L.; Bertolotti, S. G.; Previtali, C. M.; Neumann, M. G.; Encinas, M. V. *Photochem. Photobiol.* **2002**, *76*, 385–390. (c) Flamigni, L.; Venuti, E.; Camaioni, N.; Barigelletti, F. *J. Chem. Soc., Faraday Trans.* **1989**, *85*, 1935–1943.

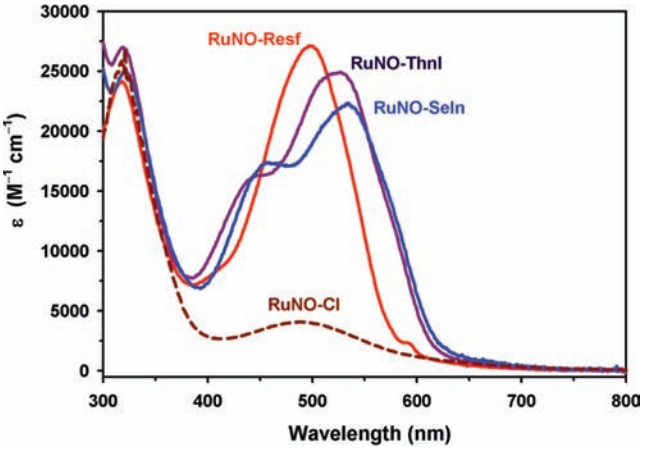

Figure 7. Electronic absorption spectra of **RuNO-Cl**, **RuNO-Resf**, **RuNO-Thnl**, and **RuNO-Seln** in $CHCl_3$ solution at 298 K.

observed when the deprotonated dyes are coordinated to the metal center (a Lewis acid) of the $\{(OMe)_2bQb)Ru(NO)\}$ moiety (vide infra). The reduced ε-values presumably arise from decrease in symmetry upon going from the basic form of the dyes (with negative charge delocalized across the tricyclic ring structure) to the protonated form. Since methylation of the phenolato-O center of $Resf^-$ also blue-shifts its absorption maximum (to 460 nm) and lowers the intensity of the absorption band (16 200 M^{-1} cm^{-1}), it is evident that interaction of proton (or the metal center) with the phenolato-O center of $Resf^-$ is actually responsible for the observed changes. A close look at the bottom panel of Figure 6 reveals another interesting observation in relation to the heavy-atom substitution in the dye frame. In case of Thnl (S) and Seln (Se), a second absorption feature appears around 425 nm. This additional feature in case of the latter two dyes is an intrinsic one and is also noted in the electronic absorption spectra of the corresponding nitrosyl-dye conjugates (vide infra).

RuNO-Cl. In $CHCl_3$ solution, the parent nitrosyl $[((OMe)_2bQb)Ru(NO)(Cl)]$ (**RuNO-Cl**) exhibits a low-intensity absorption band centered at 500 nm ($\varepsilon = 4\,950$ M^{-1} cm^{-1}; Figure 7, dashed dark red line). This feature arises from a $d_\pi(Ru) \rightarrow \pi^*(NO)$ transition[47] which is thought to give rise to the observed photolability of the Ru-NO unit[45,47−49] (and hence called photoband). The much larger absorbance band in the UV region centered at 320 nm is attributed to transitions associated with the ligand frame, as is typically observed in other metal complexes derived from quinoline-based ligands. It should be noted here that we have chosen $(OMe)_2bQb^{2-}$ as the ligand, since it affords the nitrosyl **RuNO-Cl** that exhibits its photoband at the lowest energy (500 nm) compared to all other $\{Ru\text{-}NO\}^6$ nitrosyls reported so far. This nitrosyl is therefore the ideal candidate for photosensitization with new exogenous chromophores like Thnl and Seln which also exhibit strong absorption in the 500−600 nm region.

Nitrosyl-Dye Conjugates. Details of the absorption parameters of $[((OMe)_2bQb)Ru(NO)(Resf)]$ (**RuNO-Resf**) in DMF have been published before.[28] In this work, data on all three conjugates have been collected (and compared) in $CHCl_3$.

RuNO-Resf. This nitrosyl, derived from the O-atom chromophore Resf, dissolves in $CHCl_3$ to give a bright red solution. The solution displays a strong absorption band at 505 nm (Figure 7). Close inspection of Figure 7 indicates a strong overlap of the photoband of **RuNO-Cl** with the absorption band of the coordinated $Resf^-$ unit in **RuNO-Resf**. As discussed above, direct attachment of the $Resf^-$ moiety to the Ru center of the nitrosyl results in blue-shift of the dye band and allows effective overlap with the photoband of the nitrosyl moiety.

RuNO-Thnl. This nitrosyl-dye conjugate, derived from the S-atom containing chromophore thionol (Thnl), exhibits absorption features that are red-shifted compared to its O-atom chromophore congener. **RuNO-Thnl** displays its absorption maximum at 525 nm, and its intensity ($\varepsilon = 25\,000$ M^{-1} cm^{-1}) is comparable to that of **RuNO-Resf**. In addition, there is a shoulder at 440 nm. This second absorption feature is analogous to the shoulder observed in the electronic absorption spectrum of Thnl under acidic conditions (DMF/AcOH; see Figure 6, bottom panel). As discussed above, this feature is not observed in case of **RuNO-Resf** (or Resf under acidic conditions) and appears to be associated with an internal charge-transfer band of the chromophore unit. As shown in Figure 7, the low-intensity absorption band of the $\{Ru\text{-}NO\}^6$ moiety of **RuNO-Thnl** lies well under the umbrella of the absorption band of the bound chromophore. In addition, the broader absorption band of the bound chromophore allows absorption of more light in the visible range by **RuNO-Thnl** compared to **RuNO-Resf**.

RuNO-Seln. This nitrosyl-dye conjugate, derived from the novel heavy-atom chromophore Selenophore (Seln), exhibits absorption properties similar to its sulfur-containing Thnl analogue described above. The λ_{max} value of **RuNO-Seln** is red-shifted further to 535 nm (Figure 7), and the intensity of the dye band is reduced to some extent ($\varepsilon = 22\,400$ M^{-1} cm^{-1}). The second absorption feature of the Seln dye is observed at 460 nm. Although the absorption parameters of **RuNO-Thnl** and **RuNO-Seln** do not differ much (Figure 7), the extent of NO photolability (i.e., photosensitivity) of these two nitrosyl-dye conjugates is very different and provides a more suitable basis for differentiating the effects of S- versus Se-containing chromophore.

NO Photolability and Photosensitization. RuNO-Cl. Upon exposure to visible light ($\lambda > 465$ nm, 300 mW), a solution of the parent nitrosyl **RuNO-Cl** in MeCN undergoes slow changes in its electronic spectrum (Figure S2, Supporting Information). Measurements with NO-sensitive electrode confirm that the changes are associated with photorelease of NO from **RuNO-Cl** under such illumination.[26−28,47−49] The light-driven liberation of NO is accompanied by the formation of a Ru(III) photoproduct, namely, $[((OMe)_2bQb)Ru(MeCN)(Cl)]$, which exhibits a low-energy

(47) (a) Works, C. F.; Jocher, C. J.; Bart, G. D.; Bu, X.; Ford, P. C. *Inorg. Chem.* **2002**, *41*, 3728–3739. (b) Works, C. F.; Ford, P. C. *J. Am. Chem. Soc.* **2000**, *122*, 7592–7593.

(48) (a) Sauaia, M. G.; de Lima, R. G.; Tedesco, A. C.; da Silva, R. S. *Inorg. Chem.* **2005**, *44*, 9946–9951. (b) Toledo, J. C.; Neto, B. D. S. L.; Franco, D. W. *Coord. Chem. Rev.* **2005**, *249*, 419–431. (c) Tfouni, E.; Krieger, M.; McGarvey, B. R.; Franco, D. W. *Coord. Chem. Rev.* **2003**, *236*, 57–69.

(49) Prakash, R.; Czaja, A. U.; Heinemann, F. W.; Sellmann, D. *J. Am. Chem. Soc.* **2005**, *127*, 13758–13759.

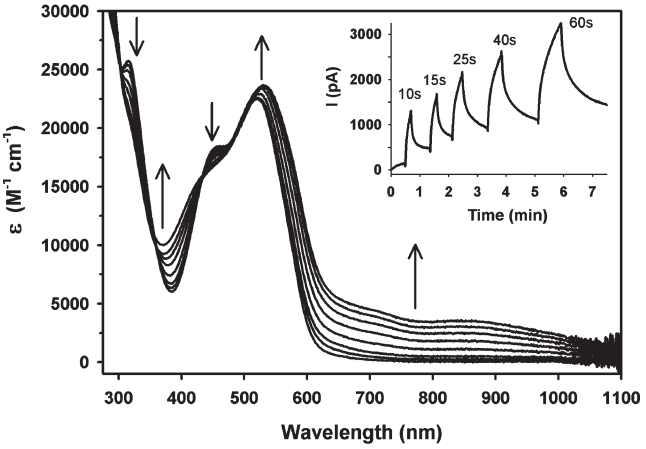

Figure 8. Changes in the electronic absorption spectra of **RuNO-Seln** in MeCN upon illumination with intervals (30 s to 5 min) of red light ($\lambda_{irr} \geq$ 585 nm; 200 mW). The final two traces were obtained upon exposure to 5 min of broad visible light ($\lambda_{irr} \geq$ 500 nm; 300 mW). Inset: NO amperogram of **RuNO-Seln** in MeCN/H_2O (1:1) upon illumination with red light for time periods as indicated.

band near 650 nm. This low-energy transition has been assigned to a ligand-to-metal charge transfer (LMCT) band arising from the negatively charged ligand (in this case, $(OMe)_2bQb^{2-}$) to the Ru(III) center.[45] The photoproduct gives a strong EPR signal, typical low-spin d^5 system, in MeCN/toluene frozen glass at 125 K ($g = 2.48, 2.25, 1.79$). Quantum yield measurements at 500 nm indicate that **RuNO-Cl** releases NO in MeCN with $\phi_{500} = 0.025$, a value higher than its closely related congener [(Me_2bpb)Ru(NO)(Cl)] ($\phi_{500} < 0.01$).

RuNO-Resf and RuNO-Thnl. We have previously reported that direct attachment of the Resf dye to the {$(OMe)_2bQb$)Ru(NO)} moiety in **RuNO-Resf** enhances its quantum yield (ϕ_{500}) to ~0.20, a marked improvement compared to its dye-free congener **RuNO-Cl**.[28] In this work, we compare the quantum yield of this nitrosyl-dye conjugate with those of two new ones that contain analogous dyes with heavy-atom substitution. Exposure of a solution of **RuNO-Thnl** in MeCN to low-intensity 500 nm light (300 mW) causes changes in its electronic absorption spectrum (Figure S3, Supporting Information) analogous to those observed with **RuNO-Resf**. Clean isosbestic points at 360 and 480 nm as well as generation of a new low-energy band centered at 830 nm indicates clean release of NO and formation of the Ru(III) photoproduct (strong EPR signal). The presence of the LMCT band around 830 nm and the strong dye band with λ_{max} at 500 nm confirms that the Ru(III) photoproduct is indeed [$((OMe)_2bQb)$Ru(MeCN)(Thnl)].

RuNO-Seln. Very similar changes in the electronic absorption spectra of **RuNO-Seln** (MeCN solution; Figure 8) are observed upon exposure to 500 nm (blue) light. More remarkable is the fact that this nitrosyl-dye conjugate also releases NO upon exposure to 600 nm (red) light, albeit at much lower rate. Photolysis of **RuNO-Seln** in MeCN with filtered red light ($\lambda_{irr} \geq$ 600 nm; 200 mW) generates a broad low-energy band from 800 to 1000 nm because of formation of the photoproduct [$((OMe)_2bQb)$Ru(MeCN)(Seln)] (strong EPR signal with $g = 2.24, 2.19, 1.88$). Quite in contrast, no change in the electronic absorption spectrum is noted when solution of either **RuNO-Thnl** or **RuNO-Resf** is irradiated with the same red light.

To make a quantitative comparison of the four nitrosyls, **RuNO-Cl**, **RuNO-Resf**, **RuNO-Thnl**, and **RuNO-Seln**, we have determined their quantum yields of NO photorelease (in MeCN) upon exposure to lights of various wavelengths in the 500−600 nm range. The results of such measurements are summarized in Table 3. The quantum yield values of some other metal nitrosyls (in different solvents), reported by other groups, are also listed for the sake of comparison. A clear trend of increasing photosensitivity at longer wavelengths is observed upon going from **RuNO-Cl** to **RuNO-Resf** to **RuNO-Thnl** to **RuNO-Seln**. For example, while **RuNO-Resf** is not photosensitive to 550 nm light ($\phi_{550} \leq 0.01$), both **RuNO-Thnl** and **RuNO-Seln** photorelease NO with ϕ_{550} values of 0.13 and 0.17, respectively. Remarkably, **RuNO-Seln** exhibits photosensitivity all the way to 600 nm ($\phi_{600} \sim 0.04$, Table 3). A close look at Figure 7 at this point provides insight into the enhanced photosensitivity of **RuNO-Thnl** compared to **RuNO-Resf**. The broader and intense absorption of the attached Thnl dye sensitizes **RuNO-Thnl** toward 550 nm light while the narrow absorption of Resf dye fails to promote NO photorelease at this wavelength. The extent of photosensitization tails off rather quickly in case of **RuNO-Resf**. Figure 7 also reveals that the absorption spectra of **RuNO-Thnl** and **RuNO-Seln** are very similar to each other. The fact that **RuNO-Seln** is still a better-sensitized nitrosyl-dye conjugate supports the so-called "heavy-atom chromophore effect" often mentioned in the area of photosensitization. We have attempted to look further into the origin of the enhanced photosensitivity of **RuNO-Seln** in our theoretical work as described below.

DFT Calculations. To elucidate the reason(s) behind variations in the extent of photosensitization by the three dyes, we have performed a DFT study on all four nitrosyls **RuNO-Cl**, **RuNO-Resf**, **RuNO-Thnl**, and **RuNO-Seln** using the B3PW91 hybrid functional and 6-31G* basis set for light atoms (C, H, N, O, S). For Ru, the Stuttgart ECP basis set was employed while the 6-311G* basis set was used for Se in case of **RuNO-Seln**. The B3PW91 approach has been shown to outperform other hybrid functionals like B3LYP or pure functionals like PW91 in numerous cases for ruthenium,[40,50,51] especially when ligated to back-bonding ligands like CO or NO.[41] Because DFT is essentially a ground-state theory, the following discussions should serve only as a theoretical model (and a potential explanation) for the NO photolability of the nitrosyl-dye conjugates.

The MO energy level diagram in Figure 9 summarizes the electronic configuration of the parent nitrosyl **RuNO-Cl** and the simplest nitrosyl-dye conjugate **RuNO-Resf**. In the occupied manifold of **RuNO-Cl** (Figure 9, lower left), the HOMO ($E = -4.60$ eV) is dominated by a ligand-based orbital derived from the negatively charged carboxamido-N moiety delocalized across the conjugated

(50) Ayed, T.; Barthelat, J.-C.; Tangour, B.; Pradére, C.; Donnadieu, B.; Grellier, M.; Sabo-Etienne, S. *Organometallics* **2005**, *24*, 3824–3826.
(51) (a) Hratchian, H.; Milleti, M. C. *J. Mol. Struct.: THEOCHEM* **2005**, *724*, 45–52. (b) Wang, H.; Miki, E.; Re, S.; Tokiwa, H. *Inorg. Chim. Acta* **2002**, *340*, 119–126. (c) Huang, D.; Streib, W. E.; Eisenstein, O.; Caulton, K. G. *Organometallics* **2000**, *19*, 1967–1972.

Table 3. Quantum Yield (ϕ) Values of Selected Nitrosyls in the Visible Range[a]

	irradiation wavelength (λ_{irr}) in nm				
complex	500	525	550	575	600
RuNO-Cl [((OMe)$_2$bQb)Ru(NO)(Cl)]	0.025	−−	−−	−−	−−
RuNO-Resf [((OMe)$_2$bQb)Ru(NO)(Resf)]	0.124	0.078	−−	−−	−−
RuNO-Thnl [((OMe)$_2$bQb)Ru(NO)(Thnl)]	0.155	0.190	0.131	−−	−−
RuNO-Seln [((OMe)$_2$bQb)Ru(NO)(Seln)]	0.189	0.214	0.176	0.152	0.040
Other Reported Nitrosyls					
[(Me$_2$bpb)Ru(NO)(Resf)][b]	0.052	−−			
[(Me$_2$bpb)Ru(NO)(Cl)]	−−	−−			
[Ru(NH$_3$)$_5$(pz)Ru(bpy)$_2$(NO)](PF$_6$)$_5$[c]		0.025			
Roussin's Salt Ester (RSE)[d]			0.00019		
PPIX-RSE[e]			0.00025		
Fluor-RSE[f]	0.0036 (436 nm)				

[a] All ϕ-values are reported with error range of ± 0.01. Note that "−−" denotes ϕ-values of ≤0.01 in our measurements; blank entries indicate values not reported. [b] Ref 27, [c] Ref 48a, [d] Ref 19a, [e] Ref 30b, [f] Ref 30a

phenylene-diamine unit. The HOMO−1 level is composed of the corresponding perpendicular orbital, while the next occupied orbital (HOMO−2) is primarily Cl^- based. More importantly, HOMO−3 (at −6.50 eV) is composed of a large portion of a d_π(Ru) − π(NO) *bonding* interaction.[52] One must note that the NO photolability of {Ru-NO}^{6} nitrosyls is thought to arise from a d_π(Ru) → π^*(NO) MLCT transition.[47,53] It is thus likely that such a transition originates from an orbital like HOMO−3 as shown in Figure 9.[54] In the unoccupied MO manifold of **RuNO-Cl** (Figure 9, top left), the first two LUMO levels (−2.80 and −2.64 eV) of **RuNO-Cl** are primarily composed of a d_π(Ru) − π^*(NO) *antibonding* interaction, the photoexcitation to which drives Ru−N bond cleavage and thus NO photolability.[53,54] A significant extent of mixing of the d_π(Ru) − π^*(NO) with the quionoline π^* system is also observed in the first four closely spaced LUMO levels (denoted as (Q)π^* in Figure 9). Such mixing most possibly accounts for the red-shifted photoband (λ_{max}≈500 nm) observed in the quinoline-based [((OMe)$_2$bQb)Ru(NO)(Cl)] (**RuNO-Cl**), as compared to its pyridine-based congener[(Me$_2$bpb)Ru(NO)(Cl)] (λ_{max} ≈ 400 nm), which does not exhibit any mixing of the d_π(Ru) − π^*(NO) and π^*(py) orbitals. Additional unoccupied metal-based orbitals (d_{z^2} and $d_{x^2-y^2}$) are also observed at much higher energies (−1.20 and 0.76 eV) but are not shown as they are not thought to be involved in NO photolability.[53]

The MO diagram of **RuNO-Resf** is noticeably enhanced by the presence of the bound Resorufin chromophore. Although the MOs of the {((OMe)$_2$bQb)Ru(NO)} moiety remain largely unchanged when compared to **RuNO-Cl**, the MOs of the bound chromophore are now intercalated into this manifold (Figure 9, right panel). Most importantly, one new low-energy unoccupied orbital (LUMO+4) appears in the LUMO manifold (Figure 9, top right) at −2.37 eV that is composed of *the π^*(Resf) orbital and the d_π(Ru) − π^*(NO) orbital*. This finding suggests that photoexcitation of the bound Resf chromophore could lead directly to Ru−N(O) bond cleavage and would provide a suitable model for the significant increase in experimental quantum yields of NO photorelease upon dye coordination.

The occupied manifold of **RuNO-Resf** (Figure 9, bottom right) also presents some interesting results, as three new chromophore-based MOs intercalate the MOs of the {Ru-NO} moiety. First, a higher-energy HOMO−1 level (−5.33 eV) is derived from the π(Resf) system, and a second orthogonal (or perpendicular) π(Resf) orbital is observed at −6.23 eV. Transition from this π(Resf) HOMO−1 to the π^*(Resf) LUMO+4 is symmetry forbidden. In contrast, transition from the π(Resf) orbital HOMO−4 to the mixed π^*(Resf)‖d_π(Ru)-π^*(NO) level (LUMO+4) is highly favored. It is therefore evident that photoexcitation of the {π(Resf) → π^*(Resf)‖d_π(Ru)-π^*(NO)} transition (i.e., {HOMO−4→ LUMO+4} in case of **RuNO-Resf** could enhance the Ru-based {d_π(Ru)→π^*(NO)} MLCT transition ({HOMO −5→LUMO} in Figure 9, right panel) leading to greater NO photolability.

To support this proposition, we have also calculated the analogous MO energy level diagrams for **RuNO-Thnl** and **RuNO-Seln** (summarized in Figure 10). One can clearly see that while the energy of the higher π(dye) (dye = Resf, Thnl, Seln) HOMO−1 orbital remain relatively constant, the orthogonal π(dye) orbitals at lower energies are (a) *qualitatively* increased from the HOMO−4 to HOMO−2 upon substitution of S(Thnl) or Se(Seln) for O(Resf), and (b) *quantitatively*, their energies are systematically increased as one moves from **RuNO-Resf** (E = −6.23 eV) to **RuNO-Thnl** (E = −5.85 eV) to **RuNO-Seln** (E = −5.71 eV). This trend in increasing π(dye) orbital energies results in smaller energies of transition to the π^*(dye)‖d_π(Ru)-π^*(NO) orbital which decreases in the order $\Delta E = 3.86 > 3.54 > 3.40$ eV for **RuNO-Resf**, **RuNO-Thnl**, and **RuNO-Seln**, respectively. This can be correlated to the shift in λ_{max} of the coordinated dye-band from **RuNO-Resf** (λ_{max} = 500 nm) to **RuNO-Thnl** (λ_{max} = 525 nm) to **RuNO-Seln** (λ_{max} = 535 nm), as well

(52) (a) Sizova, O. V.; Lyubimova, O. O. *Russ. J. Gen. Chem.* **2004**, *74*, 996–1000. (b) Sizova, O. V.; Baranovskii, V. I.; Ivanova, N. V.; Sizov, V. V.; Ershov, A. Y.; Nikol'skii, A. B. *Russ. J. Gen. Chem.* **2002**, *72*, 1831–1839.

(53) (a) Conradie, J.; Quarless, D. A.; Hsu, H.-F.; Harrop, T. C.; Lippard, S. J.; Koch, S. A.; Ghosh, A. *J. Am. Chem. Soc.* **2007**, *129*, 10446–10456. (b) Greene, S. N.; Richards, N. G. J. *Inorg. Chem.* **2004**, *43*, 7030–7041.

(54) (a) Videla, M.; Jacinto, J. S.; Baggio, M. T.; Garland, M. T.; Singh, P.; Kaim, W.; Slep, L. D.; Olabe, J. A. *Inorg. Chem.* **2006**, *45*, 8608–8617. (b) Sizova, O. V.; Ivanova, N. V.; Sizov, V. V.; Nikol'skii, A. B. *Russ. J. Gen. Chem.* **2004**, *74*, 481–485. (c) Gorelsky, S. I.; da Silva, S. C.; Lever, A. B. P.; Franco, D. W. *Inorg. Chim. Acta* **2000**, *300−302*, 698–708.

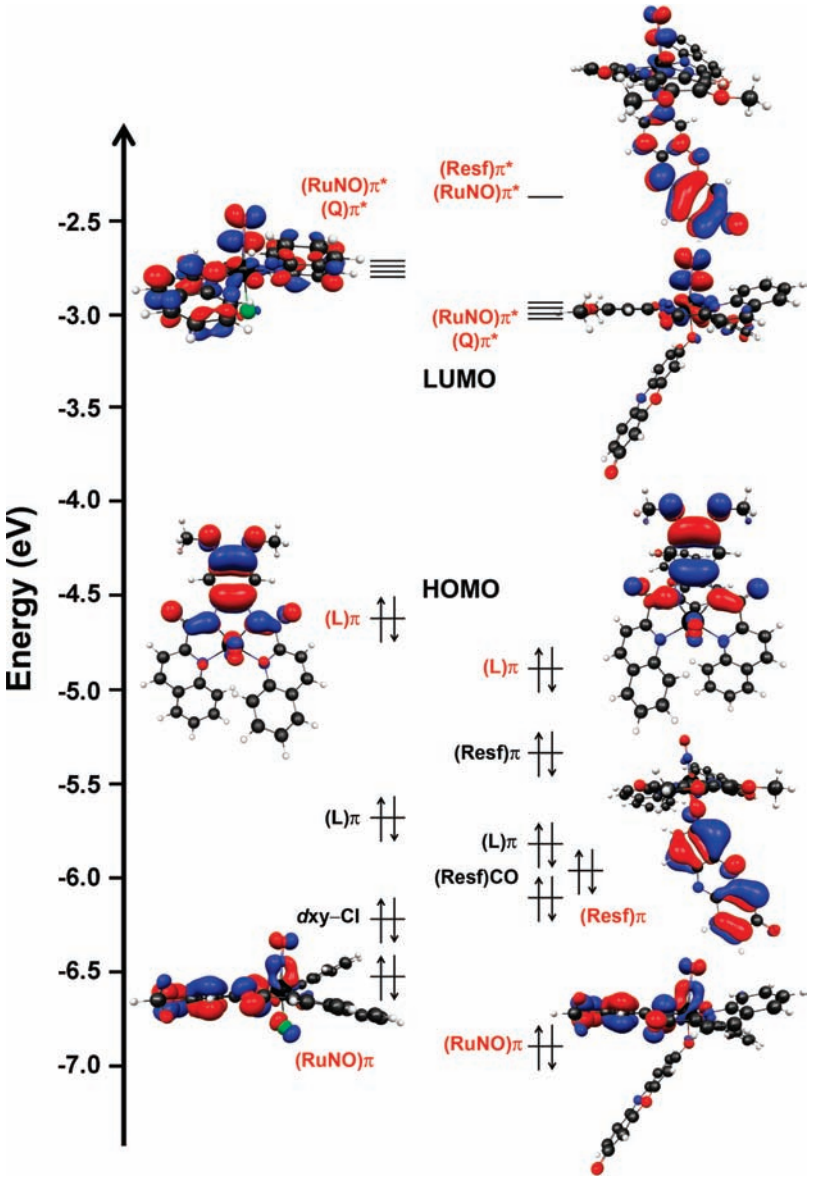

Figure 9. Calculated HOMO/LUMO diagrams for the ruthenium nitrosyl **RuNO-Cl** and its dye-conjugate **RuNO-Resf**, showing the intercalation of the chromophore HOMO/LUMO orbitals with those of the parent nitrosyl. The visually represented MO's are indicated in red in the electron configuration diagram.

as with the increased quantum yields observed with the "heavy-atom" chromophore effect. It is equally important to note that the intrinsic $d_\pi(Ru) - \pi^*(NO)$ antibonding orbital (LUMO = −2.99, −2.99, and −3.02 eV for O, S, and Se, respectively) remains unchanged across the heavy-atom series, reinforcing the notion that the occupied MO's of the coordinated dyes are the origin of low-energy photosensitization in these nitrosyl-dye conjugates.

Results of time-dependent DFT (TD-DFT) calculations also provide strong support to our conclusions. For example, the calculated electronic spectrum of **RuNO-Resf** exhibits several strong features in the ∼500 nm region, the strongest of which is a Resf(π)→RuNO(π^*) transition (Figure S5, Supporting Information). This direct electronic transition *from the coordinated dye to the RuNO moiety* is clearly responsible for the observed sensitization of the $\{Ru\text{-}NO\}^6$ nitrosyl to visible light. It also suggests that a high extent of "through-bond" energy transfer is possible when the chromophore is directly attached to the {Ru-NO} moiety. Similar trends are observed in case of both **RuNO-Thnl** and **RuNO-Seln**, albeit it at slightly lower energies (in accordance with experimental results). The TD-DFT profile of **RuNO-Cl** (Figure S4, Supporting Information) on the other hand, exhibits transitions of *relatively lower intensity* near ∼500 nm all of which originate from either the ligand(π) system in the equatorial plane (HOMO in Figure 9, left panel) or from Ru-based orbitals. In each case, the electron is excited to either pure RuNO(π^*) antibonding orbitals (HOMO + 2/ + 3) or mixed {RuNO(π^*)‖Q(π^*)} orbitals (HOMO/HOMO + 1 where Q = quinoline). Direct attachment of the chromophore introduces more allowed transitions between the highly conjugated π-system of the dye and the {Ru-NO} moiety along the Dye-Ru-NO axis. This phenomenon makes the dye-attached nitrosyls of the present study more sensitive to visible light.

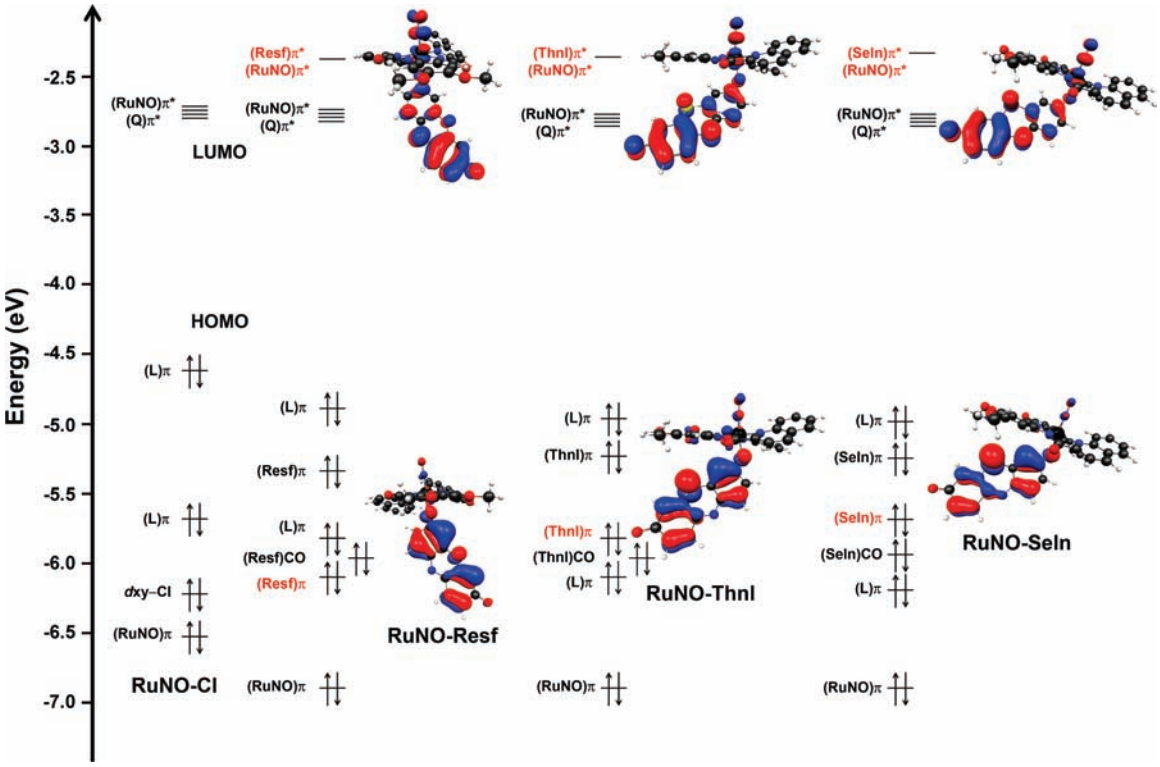

Figure 10. Calculated MO energy level diagrams for the ruthenium nitrosyl-dye conjugates derived from Resorufin (**RuNO-Resf**) and its iso-electronic heavy-atom chromophores, Thionol (**RuNO-Thnl**) and Selenophore (**RuNO-Seln**). Selected MO's are visually represented and indicated in red in the electron configuration diagram.

Overall, our DFT investigation on photoactive ruthenium nitrosyl-dye conjugates derived from a series of heavy-atom dye chromophores provides insight into the mechanism of energy transfer between the dye molecules and the {Ru-NO} moiety. It is evident that the dye- and RuNO-based MOs in the present dye-nitrosyl conjugates are intrinsically linked via chemical bonding. The success of our strategy thus lies upon a highly efficient Dexter energy transfer process.[55,56]

Conclusions

In summary, we have synthesized and structurally characterized three ruthenium nitrosyl-dye conjugates appended with the chromophores Resorufin, Thionol, and Selenophore. In all three conjugates, the deprotonated dye molecules are directly coordinated to the Ru centers. Results of spectroscopic and photochemical studies, as well as DFT calculations, lead to the following conclusions.

(1) Changes in the absorption maxima of the ligated dye molecules via alteration of the heteroatom (O, S, or Se) in the tricyclic frame allow one to bring the dye band close to the photoband of the nitrosyl moiety. In the present study, as one moves from Se to S to O, the dye band merges into the photoband of the {((OMe)$_2$bQb)Ru(NO)} unit. When the two bands coalesce in **RuNO-Resf**, the conjugate exhibits the highest molar absorptivity and significant photosensitization of the nitrosyl moiety is observed. The strategy depicted in Figure 1 is therefore a valid one.

(2) If the dye molecule includes a heavy atom (as is the case with **RuNO-Thnl** and **RuNO-Seln**), the conjugate becomes sensitive to a broader range of visible light because of broadening of the absorption band of the coordinated dye. The broadened dye band effectively increases the light harvesting process over a wider range of wavelengths.

(3) In case of **RuNO-Seln**, the presence of the heavy atom Se not only extends the NO photolability to 600 nm but also enhances the quantum yield values (Table 3) at longer wavelengths of light. The so-called heavy atom effect is thus applicable to this type of nitrosyl-dye conjugates.

(4) Results of DFT calculations on the three conjugates reveal that in each case, one of the low-lying LUMOs is composed of the π^*(dye) orbital and the d_π(Ru) $-$ π^*(NO) orbital (Figure 9). As a consequence of this coupling, photoexcitaion of the dye enhances the d_π(Ru) $-$ π^*(NO) antibonding interaction and increases the extent of NO photodissociation (improved quantum yield). Direct coordination of the dye molecule to the Ru$-$NO moiety enables such mixing of orbitals in these conjugates.

(5) DFT calculations also show that substitution of O with S and Se in the dye unit raises the energy of the π(dye) orbitals (Figure 10). As a result, photoexcitation of the dye (and concomitant

(55) (a) Jang, S.; Jung, Y.-J.; Silbey, R. *J. Chem. Phys.* **2002**, *275*, 319–332. (b) Lin, S. H.; Xiao, W. Z. *Phys. Rev. E* **1993**, *47*, 3698–3706.

(56) (a) Tanaka, I.; Tabata, Y.; Tokito, S. *J. Appl. Phys.* **2006**, *99*, 073501. (b) Faure, S.; Stern, C.; Guilard, R.; Harvey, P. D. *J. Am. Chem. Soc.* **2004**, *126*, 1253–1261. (c) Murphy, C. B.; Zhang, Y.; Troxler, T.; Ferry, V.; Martin, J. J.; Jones, W. E. *J. Phys. Chem. B* **2004**, *108*, 1537–1543.

NO photodissociation) can be achieved with lights of lower energy upon such substitution.

Acknowledgment. This work was supported by a grant from the National Science Foundation (CHE-0553405). The X-ray facility at UCSC is supported by a NSF major research instrumentation (MRI) Grant CHE-0521569. M.J.R. received a Dissertation Year Fellowship from the UCSC Graduate Division. Experimental assistance from Nicole Fry is gratefully acknowledged.

Supporting Information Available: Thermal ellipsoid plot (50% probability) of the chromophore Selenophore (Figure S1), changes in the electronic absorption spectrum upon photolysis of RuNO-Cl (Figure S2) and RuNO-Thnl (Figure S3) with visible light, TD-DFT spectra of RuNO-Cl (Figure S4) and RuNO-Resf (Figure S5), tables of DFT parameters for RuNO-Cl, RuNO-Resf, RuNO-Thnl, and RuNO-Seln (Tables S1−S6), and X-ray crystallographic data in CIF format for RuNO-Cl, RuNO-Thnl, RuNO-Seln, and Selenophore. This material is available free of charge via the Internet at http://pubs.acs.org.